Experimental and MD Simulations Study of $CaO-ZrO_2-SiO_2$ Glasses

Luisa Barbieri,[†] Valeria Cannillo,[†] Cristina Leonelli,[†] Monia Montorsi,*[,†] Piercarlo Mustarelli,[‡] and Cristina Siligardi[†]

Dipartimento di Ingegneria dei Materiali e dell'Ambiente, Università di Modena e Reggio Emilia, via Vignolese 905, 41100 Modena, Italy, and Dipartimento di Chimica Fisica−INFM, Università di Pavia, via Taramelli 26, 27100 Pavia, Italy

Received: December 9, 2002; In Final Form: April 24, 2003

Glasses belonging to the $CaO-ZrO_2-SiO_2$ ternary system were prepared by melting raw materials at 1600 °C. Several properties of the glassy materials, such as density and thermal behavior, were experimentally determined, and the results were interpreted by comparison with the structural information derived from molecular dynamics simulations and from ^{29}Si-MAS NMR. A detailed analysis of the short- and intermediate-range structure was performed to define the role played by the different atoms present in the glass formulation and to correlate the structural modifications to the macroscopic properties of this class of glasses.

Introduction

The determination and study of meltability zones in ternary phase diagrams is the first step toward the discovery of new glassy compositions. Even if phase diagrams give an idea of liquidus temperatures at the equilibrium conditions, they do not supply information regarding the melting capability that produces homogeneous glassy materials. Some 100 °C above the liquidus temperature is usually necessary to pour a homogeneous glass out of the crucible. In this work, we report an extensive study of the ternary $CaO-ZrO_2-SiO_2$ (CZS) system,[1] which has not been extensively analyzed in the literature[2,3] despite its large application in the field of materials with low expansion coefficients as well as with good mechanical and chemical resistances.[4−8]

The objective of the study was to determine new glass compositions and to investigate their properties in terms of the role covered by each oxide. With this aim, we started by melting five different binary compositions, falling between the lowest melting eutectics in the range of 1436 and 1460 °C, in the system[9] $CaO-SiO_2$. Subsequently, different amounts of ZrO_2 were added to these binary compositions to obtain several ternary compositions falling in both the ZrO_2 and $CaSiO_3$ stability fields indicated in the $CaO-ZrO_2-SiO_2$ phase diagram.[3]

The glassy or crystalline nature of the materials was investigated by scanning electron microscopy (SEM) and powder X-ray diffraction (XRD). Physical and chemical properties such as density, refractive index, and the thermal behavior of the glass materials were measured by using classical techniques. The experimental data were supported by an extensive molecular dynamic simulation that requires an optimized procedure for treating ZrO_2-related input. This allows us to define the structural modifications responsible for the macroscopic properties shown by the glasses. A detailed characterization of the glass structure was provided, and the short and intermediate order resulting from MD simulations was discussed by comparison with standard ^{29}Si MAS NMR data to investigate the role played by the different oxides in the glass network.

Experimental Section

Five base compositions B1, B2, B3, B4, and B5 belonging to the $CaO-SiO_2$ binary system and containing different SiO_2/CaO ratios of 1.70, 1.40, 1.03, 0.80, and 0.68 were prepared. Subsequently, different amounts of ZrO_2 (5, 10, 15, 20 wt %) were added to the base compositions to obtain several ternary compositions (Table 1) falling in both the wollastonite and zirconia stability fields of the $CaO-ZrO_2-SiO_2$ diagram (selected zone in Figure 1). Mixtures of each composition containing reagent-grade calcium carbonate ($CaCO_3$ 100%), silica (SiO_2 99.9%), and zirconium silicate ($ZrSiO_4$ 99.9%) as raw materials were melted in platinum crucibles in an electric furnace (Lenton, model EHF 17/17) at 1600 °C for 30 min soaking time. The melted batches were quenched in a graphite mould to obtain small pieces of glass having a bar form and in water to obtain frits.

X-ray diffraction (XRD) was performed on finely ground specimens. Patterns were collected using a powder diffractometer (Philips PW3710) with Ni-filtered Cu Kα radiation in the 2Θ range from 10 to 50° with a step size of 0.02° and a 3-s time step. SEM observations were performed (Philips, XL 40) on superficially polished gold-coated specimens. Energy dispersion X-ray spectroscopy, EDS (EDAX PV9900), with the detector mounted on the SEM apparatus, was used to identify the chemical composition of the different phases in the samples. Because several samples after quenching present liquid/liquid phase separation or crystal separation, only the glass materials were further characterized.

The densities of the glass specimens were measured with a helium pycnometer (Micromeritics, model AccuPyc 1330) on five different samples for each glass composition. In processing the experimental data, the molar volume of oxygen (V_0) was calculated to acquire information about the structural compactness.[10] The refractive index of glasses was measured using the Becke line method.[11]

* To whom corrispondence should be addressed. E-mail: montorsi.monia@unimo.it. Phone: +39-059-2056239. Fax: +39-059-2056243.

[†] Università di Modena e Reggio Emilia.

[‡] Università di Pavia.

10.1021/jp022551c CCC: $25.00
Published on Web 06/17/2003

TABLE 1: Compositions of Studied Materials in wt % and mol %

	wt %			mol %		
sample	CaO	SiO_2	ZrO_2	CaO	SiO_2	ZrO_2
B1	35.40	64.60		36.99	63.01	
B1SZ5	33.72	61.52	4.76	36.14	61.54	2.32
B1SZ10	*32.18*	*58.72*	*9.10*	*35.31*	*60.15*	*4.54*
B1SZ15	30.78	56.18	13.04	34.53	58.81	6.66
B1SZ20	29.50	53.83	16.67	33.78	57.53	8.69
B1SZ25	28.32	51.68	20.00	33.06	56.31	10.63
B1SZ30	27.23	49.70	23.07	32.37	55.14	12.49
B2	*40.00*	*60.00*		*41.67*	*58.33*	
B2SZ5	*38.10*	*57.14*	*4.76*	*40.71*	*56.98*	*2.31*
B2SZ10	*36.35*	*54.55*	*9.10*	*39.78*	*55.70*	*4.52*
B2SZ15	*34.78*	*52.18*	*13.04*	*38.90*	*54.46*	*6.64*
B2SZ20	*33.33*	*50.00*	*16.67*	*38.06*	*53.28*	*8.66*
B2SZ25	32.00	48.00	20.00	37.25	52.15	10.60
B3	47.50	52.50		49.22	50.78	
B3SZ5	45.24	5.00	4.76	48.09	49.61	2.30
B3SZ10	*43.18*	*47.72*	*9.10*	*47.00*	*48.50*	*4.50*
B3SZ15	41.30	45.66	13.04	45.97	47.42	6.61
B3SZ20	39.58	43.75	16.67	44.98	46.40	8.62
B4	53.30	46.70		55.01	44.99	
B4SZ5	50.76	44.48	4.76	53.75	43.96	2.29
B4SZ10	*48.45*	*42.45*	*9.10*	*52.54*	*42.97*	*4.49*
B4SZ15	46.36	40.60	13.04	51.39	42.03	6.58
B4SZ20	44.42	38.92	16.66	50.29	41.12	8.59
B5	57.90	42.10		59.57	40.43	
B5SZ5	55.14	40.10	4.76	58.20	39.51	2.29
B5SZ10	52.63	38.27	9.10	56.91	38.62	4.47
B5SZ15	50.34	36.62	13.04	55.66	37.78	6.56
B5SZ20	48.25	35.08	16.67	54.47	36.97	8.56

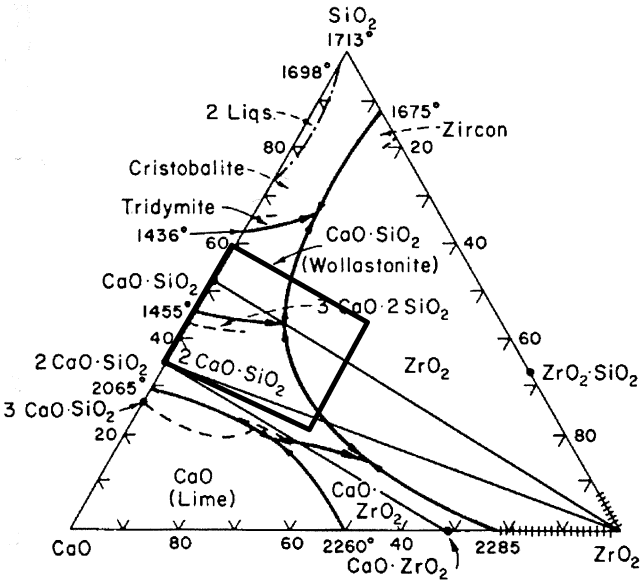

Figure 1. Compositions studied in the $CaO-ZrO_2-SiO_2$ phase diagram.

Linear expansion coefficients of glasses were obtained by using a thermodilatometer (Netzsch model EP 402) in the temperature range between 20 and 500 °C. The bars, 3.2 cm in length, were heated at 10 °C/min up to the softening point.

^{29}Si MAS NMR data were collected with a 400-MHz multinuclear FFT spectrometer ($B_0 = 9.4$ T, Bruker) at a Larmor frequency of 79.46 MHz. The spectra were acquired on freshly crushed powders by using a 7-mm probe head equipped with cylindrical zirconia rotors and a boron nitride stator. The samples were spun at 5 kHz, and the data were averaged over 500 to 1000 acquisitions using a single-pulse sequence, with a 30° pulse of 3 μs and a recycle time of 300 s. The spectra were referenced to TMS.

Computational Procedure

Several computational procedures for the simulation of glasses with high zirconia content were proposed in a previous work.[12] The computational protocol that represented the better compromise between CPU time and the prediction capability of the model was applied to the compositions considered in this work. Therefore, the starting configurations have been generated by introducing the different atoms in the simulation box in a random way, according to the chemical composition of the system reported in Table 1 (italic data). The short-range interactions between Si−O were modeled by a four-range Buckingham potential,[13] and a three-body screened Vessal potential[14] was applied to the O−Si−O linkage. The Zr−O and Ca−O interactions were codified by a simple Buckingham potential.

The starting volume of the system was expanded by up to 15% to account for the estimated thermal expansion coefficient and then scaled to reproduce the experimental density at room temperature. To reproduce an infinite solid, periodic boundary conditions were applied to the simulation box.[15] A kinetic energy corresponding to a temperature of 12 000 K was applied to the starting configuration, and the structure was cooled going thought intermediate temperatures of 10 000, 8000, 6000, 3000, 1500, and finally 300 K. At each temperature, the annealing schedule consisted of 20 000 time steps. For the first 6000 steps, the velocity was scaled every time step to reproduce the effect of a heat bath in removing the thermal energy from the system.[16] During the following 6000 time steps, the velocity was scaled every 40 time steps, whereas during the last 8000 time steps no velocity scaling was applied.

Our procedure employed the canonical NVT ensemble at high temperature, but at 3000 K, an NPT ensemble was applied using a Berendsen thermostat.[12] After having reached the temperature of 300 K, another 20 000 time steps were applied to the system, and the data were collected every 50 time steps.

The local environment of the glassy materials was analyzed in terms of the pair distribution function (PDF), which can be directly correlated to the experimentally observed bond distance and the coordination number (CN) of the different species in the glass matrix. Further information on the short-range order of the glass material can be extrapolated by the BO (bridging oxygens), NBO (nonbridging oxygens), and TBO (three bridging oxygens) distributions defined in the network of former ion−oxygen bond distance criteria: the nonbridging oxygens (NBO) are species linked to only one network former ion, the bridging oxygens (BO) are oxygens linked to two network former ions, and finally the three bridging oxygens (TBO) are oxygens linked to three network former ions.[12,17]

Further insight into the medium-range configuration of the glass structure can be achieved by the Q^n species distribution, which allows the polyhedra distribution in the glass 3D network to be described.[17]

Results and Discussion

Physico-chemical Characterization of Materials Obtained after Melting. The detailed description of the results obtained from XRD and SEM analyses is summarized in Table 2. Some of the studied compositions did not undergo melting even after being kept at 1600 °C for 30 min; others were not transparent and homogeneous, presenting a liquid−liquid or crystalline

TABLE 2: Characterization of Materials after Melting

sample	optical observations	XRD results	SEM and EDS results
B1	opaque white	amorphous	liq−liq phase separation
B1SZ5	opaque white	amorphous	liq−liq phase separation
B1SZ10	*transparent, clear, homogeneous*	*amorphous*	
B1SZ15	*transparent, clear, homogeneous*	*amorphous*	
B1SZ20	*transparent, clear, homogeneous*	*amorphous*	
B1SZ25	*transparent, clear, homogeneous*	*amorphous*	
B1SZ30	white heterogeneous	ZrO_2 crystals	crystalline + glassy phases
B2	*transparent, clear, homogeneous*	*amorphous*	
B2SZ5	*transparent, clear, homogeneous*	*amorphous*	
B2SZ10	*transparent, clear, homogeneous*	*amorphous*	
B2SZ15	*transparent, clear, homogeneous*	*amorphous*	
B2SZ20	*transparent, clear, homogeneous*	*amorphous*	
B2SZ25	white heterogeneous	ZrO_2 crystals	crystalline + glassy phases
B3	white heterogeneous	wollastonite and pseudowollastonite crystals	crystalline + glassy phases
B3SZ5	white heterogeneous	wollastonite and pseudowollastonite crystals	crystalline + glassy phases
B3SZ10	*transparent, clear, homogeneous*	*amorphous*	
B3SZ15	*transparent, clear, homogeneous*	*amorphous*	
B3SZ20	not melted		
B4	white heterogeneous	wollastonite crystals	crystalline + glassy phases
B4SZ5	white heterogeneous	wollastonite crystals	crystalline + glassy phases
B4SZ10	*transparent, clear, homogeneous*	*amorphous*	
B4SZ15	white heterogeneous	baghdadite and wollastonite crystals	crystalline + glassy phases
B4SZ20	not melted		
B5	white	larnite crystals	crystalline + glassy phases
B5SZ5	not melted		
B5SZ10	not melted		
B5SZ15	not melted		
B5SZ20	not melted		

phase separation, and the remaining compositions produced glass materials that were perfectly clear, transparent, and homogeneous.

It is worth noting that only the B2 series produced glassy materials up to 20 wt % ZrO_2. The B1, B3, B4 series presented only some glassy samples, and finally, no composition of the B5 series underwent melting. If we consider the $CaO-SiO_2$ phase binary diagram, it is possible to observe that the studied compositions fall between two low melting eutectics. Actually, B5 is a very high melting composition (about 1700 °C), and the addition of ZrO_2 does not improve the ability to obtain a glass, as shown for series B1 and B3.

Although the effects of the ZrO_2 addition to the glass sample were investigated by systematically analyzing the B2 series, the relationships among the glass properties and the different CaO/SiO_2 ratios were studied by considering the B1SZ10, B2SZ10, B3SZ10, and B4SZ10 samples.

Density measurements are more sensitive to the variations in glass composition than to any other physical property of glasses. In general, the addition of extra ions in the glass structure results in the modification of the density of the final material. In particular, this effect is strongly related to the mass of the added ions as a function of their content in the base glass.[18] The variation of the density for the B2 series induced by the zirconia addition, reported in Table 3, shows a clear increase in the experimental density as a function of the ZrO_2 concentration in the glass matrix. The trend observed for the density values does not correlate to the behavior of the V_0 parameter, which shows a shallow local minimum at 10 wt % ZrO_2. This result calls for the network-forming action of zirconium oxide, at least for relatively low molar content, in agreement with our MD and NMR findings (following discussion). However, the addition of ZrO_2 does not considerably affect the glass structure, as previously observed by a comparison between the experimental and the MD data.[19]

TABLE 3: Density Values of Studied Glasses

sample	density g/cm^3	δ	V_0 (cm^3)
B2[a]	2.796	0.001	13.196
B2SZ5[a]	2.866	0.001	12.987
B2SZ10[a]	2.995	0.001	12.648
B2SZ15[a]	3.021	0.001	12.766
B2SZ20[a]	3.057	0.001	12.709
B1SZ10[b]	2.944	0.001	12.567
B2SZ10[b]	2.995	0.001	12.648
B3SZ10[b]	3.084	0.001	12.786
B4SZ10[b]	3.068	0.005	13.265

[a] Increasing amounts of ZrO_2. [b] Increasing CaO/SiO_2 ratio.

The addition of species that fill the interstices of the vitreous network will generally increase the density. This behavior is shown for B1SZ10, B2SZ10, B3SZ10, and B4SZ10 samples, where an increase in density and a molar volume expansion with increasing amounts of CaO are observed (Table 3). This result can be explained by considering a network modifier role for the Ca atom in these glass materials, as discussed later.

The results obtained from refractive index analysis are reported in Table 4. ZrO_2 increases the refractive index of the B2 series, and this effect is due to the fact that the Zr−O bond is more polarizable than the Si−O bond, thus leading to an increased light deviation. Moreover, this result can be also interpreted in terms of glass connectivity: CaO addition promotes the breaking of the Si−O−Si bonds, thus leading to a depolymerized structure in which more $Si-O^{2-}$ Ca^{2+} species

TABLE 4: Refractive Index Values of Studied Glasses

sample	refractive index (±0.005)
B2[a]	1.600
B2SZ5[a]	1.615
B2SZ10[a]	1.630
B2SZ15[a]	1.640
B2SZ20[a]	1.650
B1SZ10[b]	1.610
B2SZ10[b]	1.630
B3SZ10[b]	1.660
B4SZ10[b]	1.660

[a] Increasing amounts of ZrO_2. [b] Increasing CaO/SiO_2 ratio.

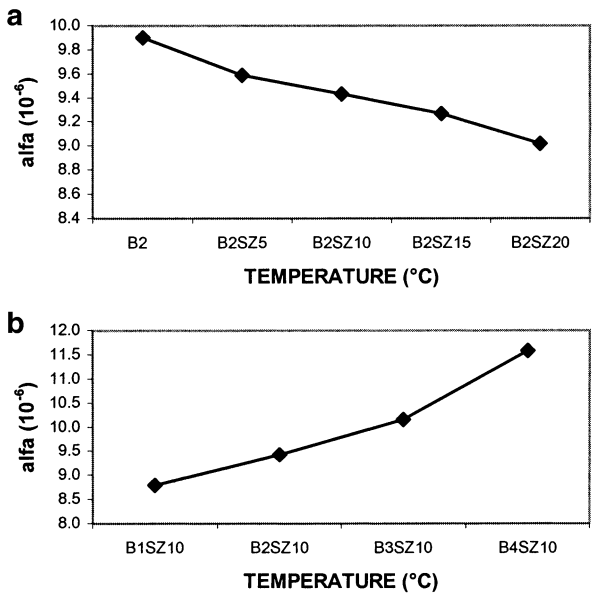

Figure 2. Thermal expansion coefficients of glasses (a) with an increasing amount of ZrO_2 and (b) with an increasing CaO/SiO_2 ratio.

are present. The presence of nonbridging oxygens is correlated to a higher refractive index of the glass materials[20] (Table 4). Both MD and NMR results confirm the increase in the NBO percentage in the glass structure as a function of the CaO addition.

The results obtained by dilatometer measurements are reported in Figure 2. The addition of ZrO_2 results in a decrease in linear expansion coefficient values, supporting a network former role played by the Zr atoms in the glass material and in agreement with the local structure obtained by MD simulation, in which the Zr−BO species represent the main contribution to the zirconium coordination (80−90%).[19] (Figure 2a) As far as the effect of the increasing addition of CaO in the glass materials is concerned, Figure 2b indicates a general increase in the α values, which is associated with a decrease in the network connectivity induced by the modifying role played by CaO.

TABLE 5: Averaged Coordination Numbers for O, Si, Zr, and Ca Atoms Obtained by MD Simulations

sample	O	Si	Zr	Ca
B1SZ10	1.56	4.03	4.97	5.66
B2SZ10	1.52	4.02	5.37	5.64
B3SZ10	1.37	4.02	5.58	5.97
B4SZ10	1.26	4.02	5.43	5.73

Computer Simulations

Bond Distances and Coordination Numbers. The pair distribution functions (pdf) for Ca−O and Ca−Ca (Figure 3) indicate bond distances in good agreement with the experimental data obtained for wollastonite. In particular, the Ca−O first-neighbor distance is 2.3 Å, which compares well to the 2.37 Å value observed for c-$CaSiO_3$.[21] Moreover, the Ca−Ca pdf shows a first peak at 3.4 Å, in agreement with the experimental value of 3.6 Å observed for crystalline wollastonite and a second peak around 6.4 Å, which provides strong evidence that zirconia-containing glasses have the same organization of crystalline $CaSiO_3$. This result, together with the averaged coordination number for Ca atoms reported in Table 5, suggests that the Ca distribution can be considered in terms of densely packed spheres in which the Ca-based octahedra are edge linked in the glassy samples, as happens in wollastonite.[21] It is worth noting that the glass local configuration reflects the structure of wollastonite, notwithstanding the fact that this material has not been used as raw a material for the synthesis of the glass samples. Further investigations of the glass network allow us to confirm the absence of peaks at around 5.3 and 7.5 Å in the Ca−Ca pair distribution function, which are associated with an out-of-plane Ca−Ca interaction and a random distribution of Ca atoms in the structure, respectively. The MD simulation shows a glass structure that is very similar to the crystalline wollastonite structure in which the CaO_6 edge-linked octahedra are connected together to approximate the cubic close packing.

Information on the local structure of the glassy materials can be also obtained by analyzing the distribution of the coordination numbers of the species present in the glass matrix. The Zr atoms present an averaged coordination of 5.34 (Table 5), in good agreement with the experimental data observed for the systems in which increasing amounts of ZrO_2 have been added.[12,19] These results indicate that Ca concentration increases in the glass composition do not produce strong modifications in the local

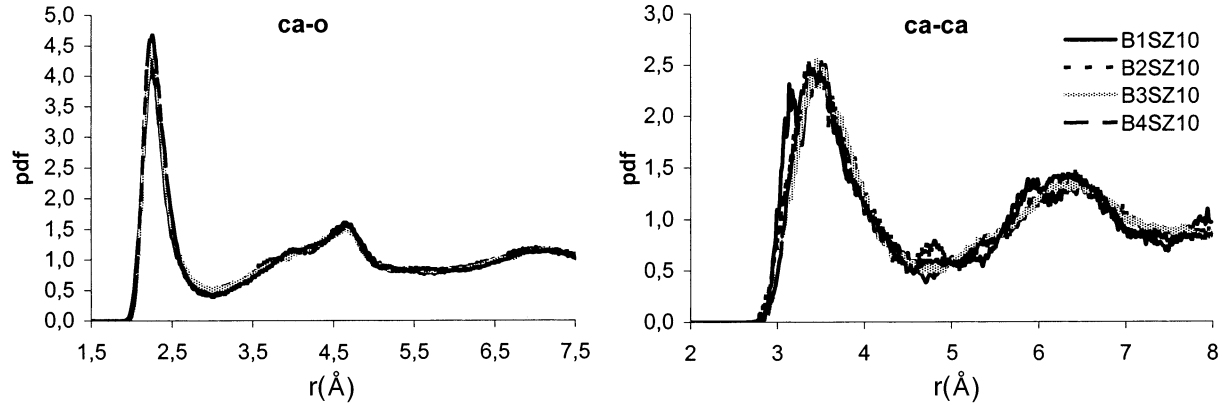

Figure 3. Pair distribution function of the Ca−O and Ca−Ca species.

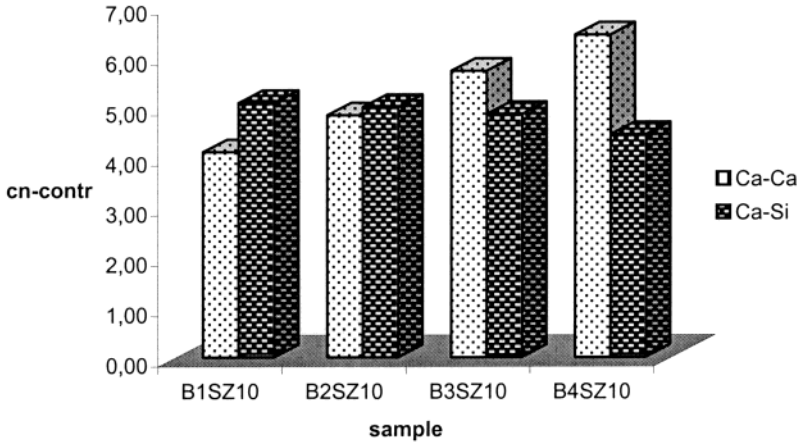

Figure 4. Contribution to the cn value of the Ca atom by Ca and Si atoms.

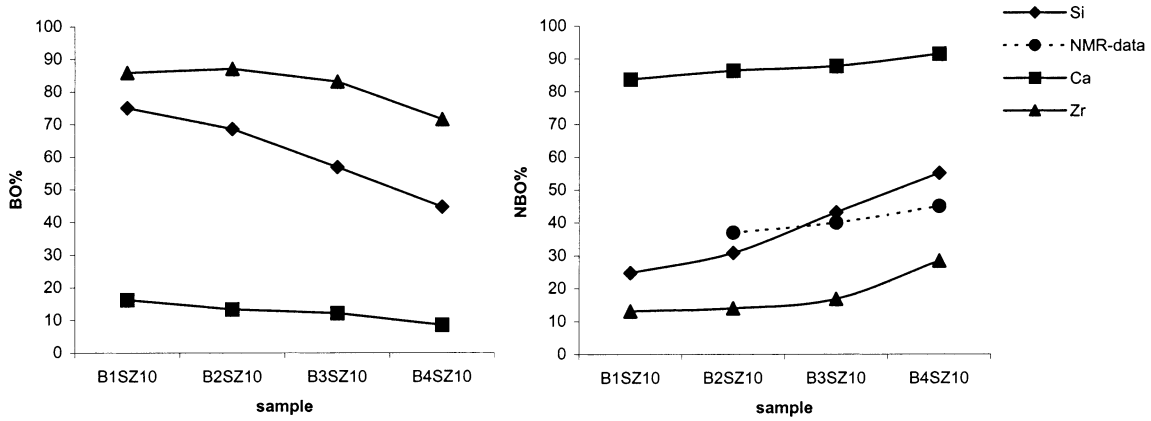

Figure 5. BO and NBO species' contribution to the coordination numbers of Si (◆), Ca (■), and Zr (▲). The NBO percentage extracted from ^{29}Si NMR is shown as a comparison for selected samples (●).

environment of Zr atoms, and the main modification induced by this atom can be observed for the Si site configuration. More evidence comes from the analysis of the contribution to the Ca coordination, which indicates that, with increasing CaO content, the Ca concentration in the calcium first coordination shell increases while silicon concentration progressively decreases (Figure 4). This result can be justified by considering that, in these glasses, Ca atoms tend to cluster together, thus promoting the progressive formation of silica-rich and alkali-rich regions, in agreement with other experimental evidence[22] on crystalline wollastonite and according to the modified continuous random network theory (MCRN).

Moreover, the analysis of the BO and NBO contributions to the calcium coordination number confirms the role of modifier played by CaO; in fact, Ca atoms surrounded by NBO species result for more than 85% (Figure 5).

The network-modifying role of the Ca atoms clearly results in the increased refractive index observed for the glass material. The effect of increasing CaO concentration in the glass network can be observed in Figure 5. In particular, the increasing amount of CaO in the glass matrix produces a more considerable decrease of the Si−BO species with respect to the Zr−BO.

Q^n Population Analysis

Further information on the Ca distribution in these glasses can be obtained by analyzing the intermediate-range order of the structure, with particular attention paid to the Q^n distribution. We recall that Q^n indicates a species in which *n* BO species are directly bonded to the network former ion.[17] This parameter allows the interpretation of how the polyhedra are linked together to form the 3D network. Figure 6a shows the Q^n distribution for the Si atoms as a function of the CaO concentration. It is possible to observe that the increased CaO concentration shifts the maximum of the peak from Q^3 species for the B1SZ10 to Q^2 for the B4SZ10, in good agreement with our MAS NMR results (Figure 7). In the latter, the main polyhedron is constituted by Si linked to 2BO and 2NBO as a result of the addition of modifier oxide in the glass network. Concerning the increasing concentration of zirconia in the glass matrix, Figure 6b shows that, for a costant Ca/Si ratio, the Si intermediate environment is not affected by the zirconium addition. This result indicates that, although the zirconium addition does not strongly modify the glass network, the CaO shows a strong capability of breaking the glass structure, thus producing large interstices in which an increasing amount of Ca is located. It is interesting to consider these results in terms of the two current models for the structure of alkali silicate glasses, namely Zachariasen's random network[23] and Greaves' MCRN.[22] In this study, the MD results support the MRN theory, and the Q^n distribution for Si atoms is in agreement with the NMR data obtained for the glass wollastonite.[24] It is also evident that the distribution of the glass-containing zirconia leads to a broader distribution with respect to the glass wollastonite. Strong experimental support of our MD results is given by standard MAS NMR ^{29}Si data as reported in the next section.

^{29}Si MAS NMR

Figure 7 shows some selected ^{29}Si MAS NMR spectra of $CaO-ZrO_2-SiO_2$ glasses. As a general consideration, they

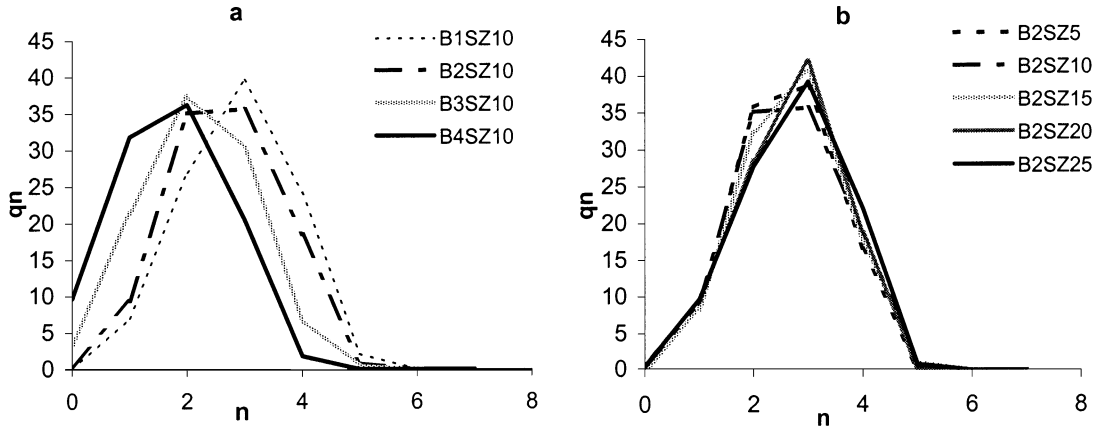

Figure 6. Q^n distribution for the Si atom for (a) an increasing CaO/SiO_2 ratio and (b) for increasing ZrO_2 content.

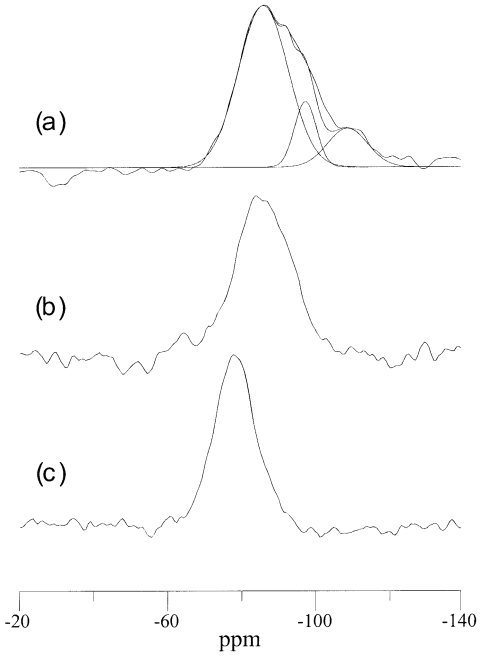

Figure 7. ^{29}Si MAS NMR spectra of the glasses (a) B2SZ10, (b) B2SZ20, and (c) B4SZ10.

become more featureless by increasing both CaO and ZrO_2. As expected, a significant shift toward the paramagnetic direction is observed for increasing CaO content. The spectra can be fitted by three Gaussian functions corresponding to Q^2, Q^3, and Q^4 structural units, whose best-fit parameters are reported in Table 6. It can be noted that the majority of silicon atoms are in Q^2 coordination, in agreement with previously reported data on glasses with similar CaO/SiO_2 ratios.[25] Because of the featureless nature of the spectra reported in the Figure, however, the deconvolution procedure we used may be somehow arbitrary, and more sophisticated double-quantum NMR techniques could be used to better investigate the connectivity of glasses.[23]

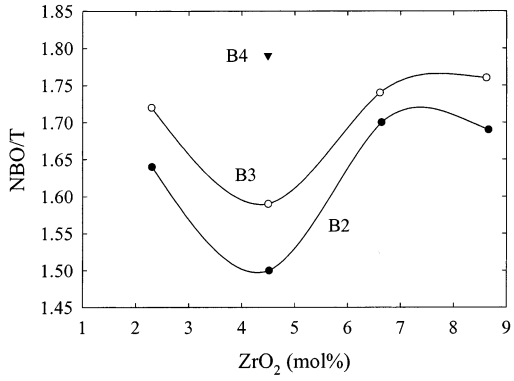

Figure 8. Number of NBOs per silicon atom vs ZrO_2 content for different B series, as determined by ^{29}Si MAS NMR. The lines are only a guide to the eye.

Effects of CaO on the Silica Matrix

The increase in CaO at constant ZrO_2 content determines a generalized increase of the Q^2 groups at the expenses of Q^3 and Q^4 which corresponds to a shift to the right for the equilibrium

$$Q^3 \leftrightarrow Q^2 + Q^4$$

This is consistent with the modifying role played by CaO in oxide glasses.[26] In particular, Figure 8 shows the number of nonbridging oxygens per silicon atom estimated on the basis

TABLE 6: Deconvolution Parameters of ^{29}Si MAS NMR Spectra

	Q^2			Q^3			Q^4		
sample	chemical shift (ppm)	fwhh[a] (ppm)	area (%)	chemical shift (ppm)	fwhh[a] (ppm)	area (%)	chemical shift (ppm)	fwhh[a] (ppm)	area (%)
B2SZ5	−85.3	19	73	−99.2	10	18	−105.2	7	9
B2SZ10	−84.2	17	61	−96.1	13	27.5	−103.2	10	11.5
B2SZ15	−84.2	17	81.5	−93.4	10	8.5	−101.6	8	10
B2SZ20	−84.9	16	78	−94.5	11	14	−102.5	8	8
B3SZ5	−79.8	19	82	−93.0	11	8	−99.6	8	10
B3SZ10	−79.1	12	72	−87.7	13	15	−93.2	6	13
B3SZ15	−79.3	13	82	−86.6	10	10	−93.2	5	8
B3SZ20	−79.8	14	84	−87.6	10	8	−93.8	5	8
B4SZ10	−77.7	12	84	−87.2	10	11	−91.4	5	5

[a] fwhh: full width at half height.

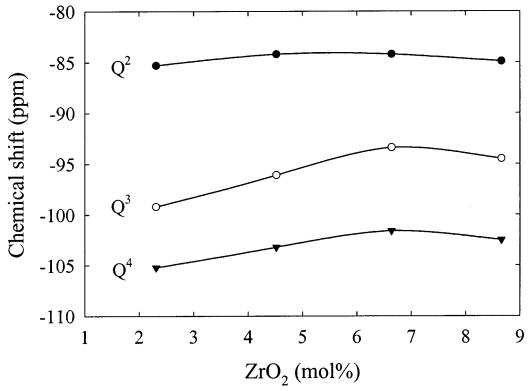

Figure 9. ^{29}Si NMR chemical shifts of Q^n units vs ZrO_2 content for some B2 glasses. The lines are only a guide to the eye.

of the data of Table 1. As expected, this value increases for increasing CaO, in good qualitative agreement with the MD results. The NBO percentage extracted from the NMR data is in agreement with the MD simulations. As an example, some points referring to samples with 10% wt zirconia are shown in Figure 5. Concerning the behavior of the chemical shifts reported in Table 6, we stress here that the paramagnetic shift displayed by the three Gaussian components when going from the B2 to B4 series likely reflects an overall paramagnetic (i.e., less shielded) shift of the spectrum because of the increasing number of NBOs.

Effects of ZrO_2 on the Silica Matrix

Figure 8 shows the nonlinear behavior of the number of NBOs per silicon atom versus the ZrO_2 molar fraction. For low content, zirconium oxide seems to exert a repairing action on the modified silica matrix that is similar to what happens with intermediate oxides such as Al_2O_3. As a matter of fact, our MD simulations show that a significant fraction of Zr atoms are in tetrahedral coordination, which is considered to be a good prerequisite to envisage a glass-forming effect.[26] For ZrO_2 contents higher that 5−6 mol %, this effect disappears. It is not clear at this moment if this is due to clustering of zirconium oxide.

Further information can be obtained by considering the chemical shifts. Figure 9 shows that the Si atoms in the most polymerized environments Q^3 and Q^4 are more affected (i.e., have increasing chemical shifts) than Q^2 by the addition of ZrO_2. Similar results were reported by Maekawa et al. on the system $Na_2O-Al_2O_3-SiO_2$[27] and were explained in terms of a higher acidity of Al_2O_3 with respect to SiO_2. However, this effect levels off for the highest ZrO_2 contents, again pointing toward a change in the chemical interactions between SiO_2 and ZrO_2.

Conclusions

In this paper, we reported the physico-chemical, MD, and ^{29}Si MAS NMR characterizations of many glassy compositions belonging to the $CaO-ZrO_2-SiO_2$ ternary system. In particular, by means of an "educated" combination of modeling and spectroscopic data, we were able to strongly substantiate short- and medium-range indirect information obtained by bulk quantities such as density, refractive index, and expansion coefficients. Our main findings are the following:

ZrO_2 plays an intermediate role in the interaction with the glassy matrix. In detail, zirconium oxide acts as a network former up to molar contents on the order of 5−10%. Its role at higher contents is not completely clear, and partial clustering cannot yet be ruled out.

As expected, CaO works as a network modifier. The addition of large amounts of CaO leads to the clustering of ions, in agreement with the modified continuous random network approach.

References and Notes

(1) Morey, G. W.; Bowen, N. L. *J. Soc. Glass Technol*. **1925**, *9*, 232.
(2) Matsumoto, K.; Sawamoto, T.; Koide, S. *Asahi Garasu Kenkyu Hokoku* **1954**, *4*, 8.
(3) Kordyuk, R. A.; Gul'ko, N. V. *Dokl. Akad. Nauk SSSR* **1962**, *142*, 640. Kordyuk, R. A.; Gul'ko, N. V. *Dokl. Chem. Technol.* **1962**, *142*, 6.
(4) Siligardi, C.; D'Arrigo, M. C.; Leonelli, C.; Pellacani, G. C.; Cross, T. E *J. Am. Ceram. Soc.* **2000**, *4*, 83.
(5) Leonelli, C.; Siligardi, C.; Agrawal, D.; Fang, Y. *Materials Research Society Symposium Proceedings*; Iskander, M. F., Kiggans, J. O., Bolomey, J. C., Eds.; Materials Research Society: Pittsburgh, PA, 1996; Vol. 430, pp 429−34.
(6) Siligardi, C.; D'Arrigo, M. C.; Leonelli, C. *Ceram. Bull.* **2000**, *79*, 88.
(7) Generali, E.; Baldi, G.; Ferrari, A. M.; Leonelli, C.; Manfredini, T.; Siligardi, C.; Pellacani, G. C. *Int. Ceram. J.* **1996**, *25*, 16.
(8) Siligardi, C.; Veronesi, P.; Leonelli, C.; Settembre Blundo, D.; Baldi, G.; Generali, E. *Tile Brick* , in press.
(9) Muan, P. *J. Am. Ceram. Soc*. **1959**, *42*, 414.
(10) Navarro, J. M. F. *El Vidrio*, 2nd ed.; Consejo Superior de Investigaciones Cientificas: Madrid, 1991; p 373.
(11) Simmons, C. J.; El-Bayoumi, O. H. *Am. Ceram. Soc*. **1993**, 14.
(12) Montorsi, M.; Menziani, M. C.; Leonelli, C.; Du, J.; Cormack, A. N. *Phys. Chem. Glasses* **2002**, *43*, 145.
(13) Smith, W.; Forester, T. R. *J. Mol. Graphics* **1996**, *14*, 136.
(14) Vessal, B.; Amini, M.; Fincham, D.; Catlow, C. R. A. *Philos. Mag. B* **1989**, *60*, 753.
(15) Cormack, A. N.; Du, J. *J. Non-Cryst. Solids* **2001**, *283*, 293.
(16) Huang, C.; Cormack, A. N. *J. Chem. Phys*. **1991**, *95*, 3634.
(17) Cormack, A. N.; Cao, Y. *Mol. Eng*. **1996**, *6*, 183.
(18) Volf, M. B. Chemical Approach to Glass. *Glass Science and Technology*; Elsevier: New York, 1984; Vol. 7, p 307.
(19) Lancellotti, I.; Leonelli, C.; Montorsi, M.; Pellacani, G. C.; Siligardi, C.; Meneghini, C. *Phys. Chem. Glasses* **2002**, *43C*, 1.
(20) Scholze, H. *Le Verre: Nature, Structure et Proprietes*. Institut du Verre: Paris, 1980.
(21) Gaskell, P. H.; Eckersley, M. C.; Barnes, A. C.; Chieux, P. *Nature* **1991**, *350*, 675.
(22) Greaves, G. N. *J. Non-Cryst. Solids* **1985**, *71*, 203.
(23) Olivier, L.; Yuan, X.; Cormack, A. N.; Jager, C. *J. Non-Cryst. Solids* **2001**, *293*−*295*, 53.
(24) Schneider, J.; Mastelaro, V. R.; Panepucci, H.; Zanotto, E. D. *J. Non-Cryst. Solids* **2000**, *273*, 8.
(25) Engelhardt, G.; Nofz, M.; Forkel, K.; Wihsmann, F. C.; Magi, M.; Samoson, A.; Lippmaa, E. *Phys. Chem. Glasses* **1985**, *26*, 157.
(26) Varshneya, A. K. *Fundamentals of Inorganic Glasses*; Academic Press: San Diego, CA, 1994.
(27) Maekawa, H.; Maekawa, T.; Kawamura, K.; Yokokawa, T. *J. Phys. Chem*. **1991**, *95*, 6822.